2007 IEEE International Conference on
Robotics and Automation
Roma, Italy, 10-14 April 2007

Simple Muscle Models Regularize Motion in a Robotic Leg with Neurally-Based Step Generation

Brandon L. Rutter, *Member, IEEE,* William A. Lewinger, *Member, IEEE*, Marcus Blümel, Ansgar Büschges, Roger D. Quinn

Abstract— **Robotic control systems inspired by animals are enticing to the robot designer due to their promises of simplicity, elegance and robustness. While there has been success in applying general and behaviorally-based knowledge of biological systems to control, we are investigating the use of control based on known and hypothesized neural pathways in specific model animals. Neural motor systems in animals are only meaningful in the context of their mechanical body, and the behavior of the system can be highly dependent on nonlinear and dynamic properties of the mechanical part of the system. It is therefore reasonable to believe that to reproduce behavior, the physical characteristics of the biological system must also be modeled or accounted for. In this paper we examine the performance of a robotic system with three types of muscle model: null, piecewise-constant, and linear. Results show that adding very simple models of muscle properties at a single joint cause marked improvement in the performance of a neurally-based step generator for a 3-degree-of-freedom robotic leg.**

I. Introduction

BIOLOGICAL systems have been a source of inspiration for robotic applications at varying levels of abstraction. In the design of legged machines this has ranged from the highly abstracted Whegs™ [1] and RHex[2] vehicles, through less abstract but still highly simplified systems like MechaRoach robots [3, 4], to more flexible and complex systems, including Robot II [5, 6], the TUM walking machine [7] the Tarry series [8], the Lauron series [9], and BILL-Ant-p [10, 11].

These systems use methods of varying complexity for coordination between and within the legs. In Whegs™ and MechaRoach both inter- and intra-leg coordination are accomplished through mechanical coupling. Indeed, in both Whegs™ and RHex systems the intra-leg coordination problem is solved by using single-link appendages. While these systems are outstanding in their simplicity and robustness, there is a limit to the complexity of behavior such systems can exhibit, and a corresponding limit to the complexity of locomotion tasks they can solve.

Coordination between legs to produce gaits has been successfully implemented [6, 7, 8, 11] using rules based on animal behavior [12]. Though these methods produce coordination between legs, subsystems must coordinate the motion within each leg. This has typically been done using inverse kinematics [6, 11]. While this is conceptually straightforward, dealing with dynamic environments and perturbations can be a matter of considerable effort. In addition, these methods require trigonometric and other computations which are often beyond the capability of microcontrollers found in small-scale robots. As a result, such robots are either larger, to house on-board processors, or require off-board, tethered control systems, which can limit mobility and usable range of operation. Other solutions for intra-leg coordination, e.g. by Wadden & Ekeberg [13, 14], are based on neurally-inspired pattern generators whose action can be modified by sensory input. The computational complexity of such systems can also be relatively high, however, since they require many simultaneous integrations to simulate the artificial neural dynamics.

Biomechanical studies strongly indicate that the performance of biological locomotor systems not only relies on the dynamic neuromuscular transform between the nervous and musculoskeletal systems of a walking animal, but can also profit from the contribution of specific muscle properties [15, 16]. The control methods used by the nervous system are likely to rely on these complex properties of the associated mechanical systems. This situation suggests the integration of muscle properties into the control methods used for legged robots. To the engineer of legged systems, then, it is important to determine what part of the nonlinear and dynamic properties of muscle are required for adequate system function. This paper addresses that problem.

II. Controller Design

A. The SCASM control method

In this work we are using Sensory Coupled Action Switching Modules (SCASM) for the generation of coordinated stepping motion in a robotic leg [26]. This control method is based on observation, neurobiology and modeling of the stick insect. In this animal evidence in the leg muscle control system suggests that the neuronal control can be subdivided into several central pattern generators

Manuscript received September 13, 2006. Work in the Case Biorobotics Laboratory was supported by NSF IGERT Training Grant DGE 9972747 and Eglin AFB Grant F08630-03-1-0003. The work on the stick insect walking system was supported by DFG grant Bu957/9 to AB.

B. L. Rutter and R. D. Quinn are with the Department of Mechanical and Aerospace Engineering, Case Western Reserve University, Cleveland, OH 44106 USA (216-368-5216; e-mail: b.rutter@ieee.org; rdq@case.edu)

W. A. Lewinger is with the Department of Electrical Engineering and Computer Science, Case Western Reserve University (wal4@case.edu)

M. Blümel and A. Büschges are with the Department of Animal Physiology, Institute for Zoology, University of Cologne, 5023 Cologne, Germany(marcus@hmbm.de; ansgar.bueschges@uni-koeln.de)

(CPG's). Each CPG can generate a basic alternating activity pattern in antagonistic muscles of a given leg joint even without any peripheral input [17, 18]. Experiments with pharmacological activation of the leg control network lead to the conclusion that each leg joint (ThC, CTr, FTi; see Fig. 1) can be associated with an individual CPG.

In order to be able to generate a stepping movement the activity of the three joint control CPG's must be coordinated. This coupling is achieved by means of sensory feedback [19-23]. Usually leg proprioceptors can be attributed to a specific leg segment and therefore be associated with the joint that moves this segment. The chordotonal organ for example is a stretch receptor inside the femur-tibia joint. It is able to signal parameters of joint geometry like joint angle or angular change [24]. Signals from the chordotonal organ do not only influence the CPG of the FTi joint itself [25] but also the motor-activation of the adjacent (CTr) joint [22, 23]. These inter-joint influences are an important mechanism of segment coordination.

B. Controller Abstraction

These results were the basis for developing a new model of leg movement control. In this model the control is split into three independent joint control systems. Each joint controller is a state machine and its simple task is to determine whether to be in the joint's flexion or extension state. To make this decision the joint controller has access to specific sensor data, but it has explicitly no information about the state of other joint controllers[26]. This reflects the uncoupled nature of the biological archetype.

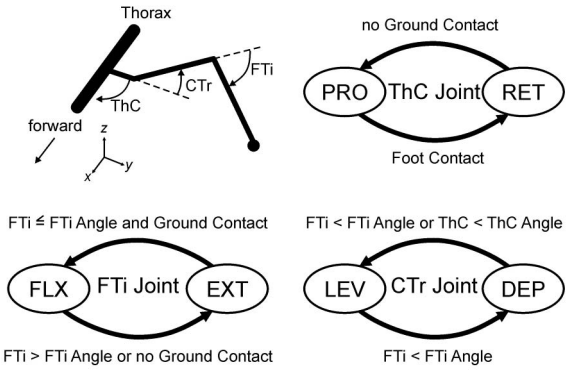

Fig. 1 Diagram of geometry and control of the simulated stick insect middle leg, showing ThC (Thoraco-Coxal) protraction and retraction, CTr (Coxa-Trochanter) levation and depression, and FTi (Femur-Tibia) flexion and extension. The conditions used by Ekeberg et al. for transitions between states are shown adjacent to each transition arrow. The leg segments, from the body outward, are the coxa, femur and tibia.

It is possible to simplify the controller's task to a set of Boolean decision rules like:

```
if (sensor-data_x > threshold_x) then
   state = flexion
else
   state = extension
```

In case of the stick insect the appropriate rules for each joint can be derived almost completely from literature; only the threshold values have to be adjusted to function with a particular leg geometry. The leg segments, from the body outward, are the coxa, femur and tibia. The trochanter is a small leg segment which is effectively fused to the femur in the stick insect, thus the coxa-trochanter joint. We maintain this nomenclature for both the stick insect scale model and the general 3-degree-of-freedom (3-DOF) leg.

III. Single-Leg Test Platform Design

We refer to the controller abstraction described above and depicted in Fig. 1 as Sensory Coupled Action Switching Modules (SCASM)[27]. In the robot described here and the simulations in [26], each joint controller comprises a module. Coordinated motion arises through the coupling of the modules through sensory information and mechanical coupling. Though they are implemented as such here, the modules need not be finite state machines; in the animal they can be considered bistable oscillators. The following section describes the implementation of the particular SCASM architecture shown in Fig. 1 on a prototype scale model of the stick insect middle leg. We consider SCASM to consist only of the mechanisms necessary for switching between various activities at the modules. These modules in turn drive the underlying plant, which in the case of this system includes muscle models.

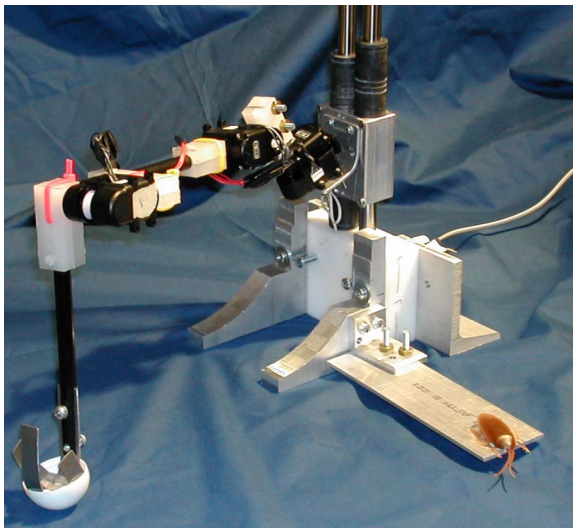

Fig. 2 Single-leg platform. This view is from the front; the bar extending to the bottom right indicates the orientation of the thorax in the horizontal plane.

The single-leg test platform, shown in Fig. 2, is a 14.3:1 scale 3-DOF model of the right middle leg of the stick insect *Carausius morosus*. Though the animal has more than one DOF at the thoraco-coxal joint, only the primary protraction/retraction DOF was used, as in the model of Ekeberg, Blümel and Büschges[26]. A smooth, low-friction foot, constructed using a half of a table-tennis ball, simulates the frictionless surface used by Ekeberg *et al.* in their modeling when used on a hard, smooth surface. The joints are actuated using AI-series servo motors from

MegaRobotics (MegaRobotics Co., Ltd. Seoul, Korea). The femur and tibia segments of this prototype were constructed from 9.5 mm diameter plastic shaft, and these are connected to the motors using adapters made from Delrin® plastic

TABLE I
JOINT ANGLES CONDITIONS FOR STATE CHANGES

Joint	State Transition	Joint Angles (degrees) ThC	FTi	CTr Load
		Sideways Stepping		
ThC	→RET	--	--	> 0.5*
	→PRO	--	--	< -0.5
CTr	→DEP		< 80*	--
	→LEV	< -25	> 115*	--
FTi	→FLX	--	≤ 100	> 0.2*
	→EXT	--	> 120*	< -1
	→EXT2†	--	< 80	<= 0
		Forward Stepping		
ThC	→RET	--	--	> 0*
	→PRO	--	--	< -0.5
CTr	→DEP	--	< 75*	--
	→LEV	< -20	> 120*	--
FTi	→FLX	--	≤ 100	> 0*
	→EXT	--	> 105*	< -1
	→EXT2†	--	< 80	<= 0

* Condition differs between restricted and forward stepping.
† Additional state implementing the piecewise-constant muscle model. This state is only enabled for tests of that model.

which interface with the standard slide-in connectors of the AI-series servomotors. The motor driving the ThC joint is connected to a body link, which is attached to the base on two vertical sliding rails used to adjust the modeled body height.

These servos are controlled via an RS-232 serial data line, and provide 8-bit angle and load feedback to the host controller over the same line. Angle feedback is used in conjunction with the servo motors' proportional control to implement a crude feed-forward torque control. For a given desired torque output, the servo is commanded to go to some delta of position from the current position; generating a torque proportional to this delta. This system generates compliant motion from an electrical motor system with relatively little computational overhead. Control is implemented on a 400 MHz Pentium-III computer running RT-Linux [28], which also records all state and sensory data for analysis and allows on-line modification of state transition conditions.

Control takes place primarily in two threads. The first of these handles the feed-forward force control and runs as quickly as it can given computation and serial communication overhead, currently 197 Hz. The second runs at a lower priority and handles the state transition and activation calculations at 100 Hz. All control and sensory data are stored in shared memory accessible both from real-time and user space, allowing online modification of the control, and data is logged via FIFO to a high-priority user space program which writes all data, including sensor readings, states and muscle activations, to files.

The state transition thread sets muscle activations based on the current state for each muscle. These activations, shown in Table II, are constant for muscles at the ThC and FTi joints. At the CTr joint the activations are dynamically set based on known activation reflexes, as was done by Ekeberg *et al.*[26].

TABLE II
MUSCLE ACTIVATION LEVELS BASED ON JOINT STATE

Joint	State	Agonist Activation	Antagonist Activation
ThC	PRO	0.6	0
	RET	1.6	0.1
CTr	LEV	Eq. (1)	0
	DEP	Eq. (2)	0
FTi (sideways)	EXT	0.6	0.09
	FLX	1.3	0.001
	EXT2	0.2	0.09
FTi (forward, piecew. const.)	EXT	0.8	0.09
	FLX	6	0.001
	EXT2	0.15	0.09
FTi (forward, linear)	EXT	0.8	0.09
	FLX	1.7	0.001

The non-constant activations in Table II are given by:

$$K_1(\text{FTi\_angle}) \quad (1)$$

$$2*K_2(\text{FTi\_angle}) + K_3(\text{CTr\_angle}) \quad (2)$$

$$K(x) = \max[0, (a + b \bullet p(x, wmin, wmax) + c \bullet q(x, wmin, wmax)] \quad (3)$$

$$p = x\text{-}wmin/(wmax\text{-}wmin);\ q=1-p \quad (4)$$

TABLE III
ACTIVATION FUNCTION PARAMETERS

K	a	b	c	wmin	wmax
1	0	0.8	0.01	61	100
2	.08	-0.205	0.008	61	100
3	0	0	0.06	-40	80

We used three types of explicit muscle model in these experiments: null, piecewise-constant, and linear.

In this work the term "linear muscle model" refers to a muscle modeled as a contractile element whose force at a particular activation is scaled by its current length. The length of the element, in turn, is determined by modeling the joint as a constant-radius pulley; the most computationally simple joint model. The linear muscle model was used only in the simulated muscles activating the FTi joint. This model of muscle activation is far simpler than those intended to accurately model muscle dynamics (e.g. that of Hill[29]), which can include parabolic, hyperbolic and exponential characteristics for both the dependence of active force on muscle length and contraction velocity, as well as passive nonlinear stiffness and damping elements.

All tests presented in this paper used the following method for computing the servo delta at each joint:

$$\Delta_{servo} = \sum_{muscles} [r \cdot f]$$
$$f = \text{activation} \cdot FL \cdot f_{\max} \quad (5)$$

where r is the radius of the pulley associated with each muscle, FL is the force-length activation scaling function, and f_{max} is a parameter intended to represent the maximum force which can be exerted by the muscle. For the null and piecewise-constant muscle models, FL was just set to 1,

eliminating the dependence of f on joint angle. For the linear muscle model, FL was a function of nondimensionalized muscle length l':

$$FL = a + b \cdot l'$$
$$l' = \frac{(\alpha - \theta) r + l_0}{l_0} \quad (6)$$

with a and b constant parameters, θ the joint angle, l_0 the "resting" length of the muscle and α the joint angle at which the muscle reaches this length. The parameters used for each muscle in the controller are given in Table IV. Note that the angle parameters are implicitly shown in radians in Eqn (6), but given in degrees in the table. Note also that the parameters given in Table IV are for muscles, not states. There is no FTi_EXT2 muscle. The EXT2 state just sets activations differently for the FTi extensor and flexor muscles.

The FTi post-extension (EXT2) state is in effect a piecewise-constant force-length characteristic for the FTi extensor muscle. It is only in effect during extension, but putting it into effect during flexion would likely have little effect due to the low extensor activity during flexion.

TABLE IV
MUSCLE MODEL PARAMETERS

Muscle	l_0	r	α	f_{max}	a	b
Sideways Stepping						
ThC_RET	--	-0.5	--	10	--	--
ThC_PRO	--	0.5	--	10	--	--
CTr_DEP	--	-1	--	10	--	--
CTr_LEV	--	1	--	10	--	--
FTi_FLX	--	1	--	10	--	--
FTi_EXT	--	-1	--	10	--	--
Forward, Piecewise Constant						
ThC_RET	--	-0.5	--	15	--	--
ThC_PRO	--	0.5	--	15	--	--
CTr_DEP	--	-1	--	10	--	--
CTr_LEV	--	1	--	10	--	--
FTi_FLX	--	1	--	20	--	--
FTi_EXT	--	-1	--	10	--	--
Forward, Linear						
ThC_RET	--	-0.5	--	18	--	--
ThC_PRO	--	0.5	--	15	--	--
CTr_DEP	--	-1	--	12	--	--
CTr_LEV	--	1	--	15	--	--
FTi_FLX	5	1	95	30	-1.5	2
FTi_EXT	5	-1	100	14	-1.4	2

Though it is not modeled explicitly and has not been quantified, there is also a force-velocity dependence inherent in the force control method used. As a joint moves more quickly in the direction it is being driven, the average distance between the commanded position and the joint's actual position will become less, reducing the torque applied to the joint. The inverse is also true; decreasing joint velocity increases force.

IV. RESULTS

We first tested the operation of the model leg in the restricted single leg preparation, which corresponds to a reduced biological preparation in which all legs but one are removed and the ThC joint of that leg is immobilized [30, 31]. This preparation allows a stepping movement sometimes called "sideways walking". During sideways stepping tests, the body link was adjusted such that the ThC joint was about 16 cm above the ground.

A. Sideways Stepping

We first compared the operation of the sideways stepping system with the null and piecewise-constant muscle models. In development of the system, it became apparent that one of the most difficult aspects of stepping control using this method is the swing-stance transition.

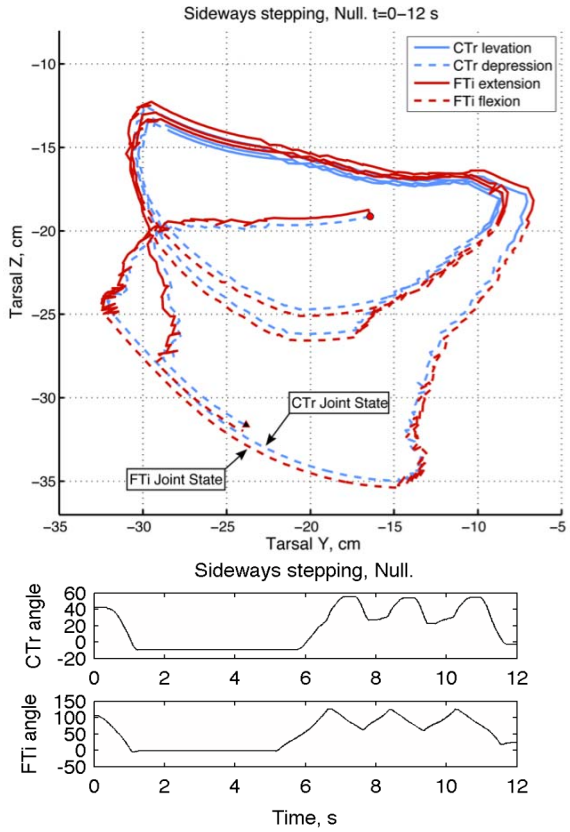

Fig. 3 Path-state plot (top) and joint trajectories in degrees (bottom) of sideways stepping with null muscle model. The path-state plot is a plot showing simultaneous foot path and joint states, and is used in several of the following figures. Each line represents the state of one joint, styled as shown in the legend. The foot path regenerated from joint angle data is represented by the line which starts at the circle and terminates at the triangle; in this case that is the line representing CTr joint state. In this and in Fig. 4, negative Y is away from the body since the model is a right leg (see Fig. 1). The origin is at the ThC joint, and this is a projection of the already nearly planar restricted stepping motion is therefore onto a transverse plane. This system ceases motion after one second due to postponed detection of ground contact, and must be brought back to the feasible range of joint angles by hand. It again detects ground contact too late at about 11.5 seconds.

On this platform one of the signals used to detect ground contact and complete this transition is load at the CTr joint. Therefore a measurable increase in load is critical for

switching to stance phase. However, with the FTi joint extending, this increase in force can be very small, since FTi extension is acting to bring the foot up while CTr depression acts to bring the foot down, and the sliding foot does not firmly engage the substrate upon contact. As shown in Fig. 3, this can result in delayed detection of ground contact, which disrupts the stepping cycle and brings the system to a halt. Introduction of the piecewise-constant muscle model at the FTi extensor makes the swing-stance transition nearly completely reliable when properly tuned.

The lack of a constant-Z portion during stance in these runs (as in forward stepping, not shown) is due to flexibility in the leg structure; precise foot position cannot be inferred accurately from measured joint angles. This information is not necessary, however, for SCASM to function.

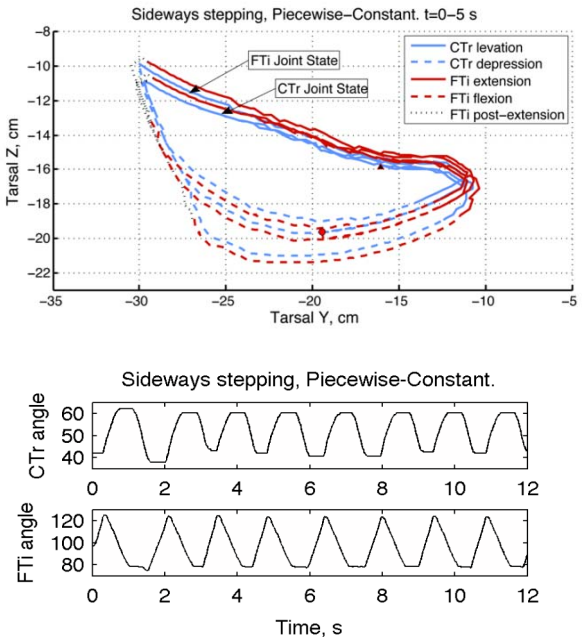

Fig. 4 Path-state plot and joint trajectories with the piecewise-constant muscle model, implemented using a third FTi "Post Extension" state. In this example the system quickly stabilizes, although "ground contact" was apparently detected before actual foot contact during two of the first three step cycles, which are depicted in the top plot.

B. *Forward stepping*

In forward stepping, motion of the ThC joint is allowed. This is the primary difference between this and restricted stepping; most other parameters of the control system can remain the same and still produce stepping, though we tuned them to produce better behavior as seen in Table I.

Forward stepping with the null muscle model fails to detect the ground and transfer to stance muscle activations on the first step; the histograms and statistics shown in Fig. 5 and Fig. 6 compare only the piecewise-constant and linear FTi muscle models. These histograms were generated from analysis of ten minutes of stepping for each of the two types of muscle model. In each case it was possible to generate reliable stepping behavior, though it took more effort to find a set of control parameters which accomplished this for the piecewise-constant case; this appeared to be due to a higher sensitivity to the transition parameters in that case. Additionally, leg motion when using the linear FTi muscle model appears smoother, but this has not been quantified.

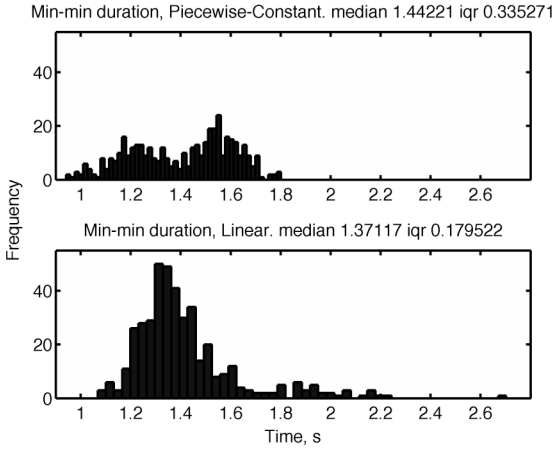

Fig. 5 Histograms showing the distributions of durations of the entire step cycle, as measured from one minimum of ThC angle to the next. The medians do not differ significantly according to the Wilcoxon test (p=0.22), and the distributions differ with $p = 1x10^{-8}$ according to the Kolmogorov-Smirinov test. Note the bimodal behavior in the piecewise-constant data.

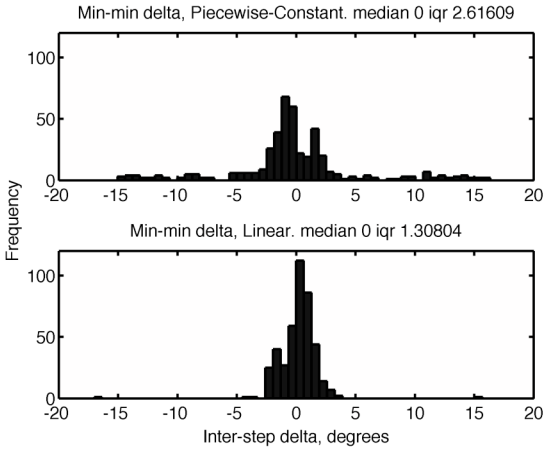

Fig. 6 Histograms showing the distributions of difference of the minimum ThC angle from step to step. The medians do not differ significantly according to the Wilcoxon test (p=0.14), but the distributions differ with $p = 3.7x10^{-5}$ according to the Kolmogorov-Smirinov test. The lack of the wide tails on data taken using the linear muscle model indicates a more consistent placement of the foot at transition from stance to swing.

V. Conclusions

In [27] we suggested that the state transition modules of SCASM must drive an underlying plant with limited actuation capability towards the extremes of the range of motion in order to ensure stable ongoing generation of the desired repetitive motion sequence. Here we have demonstrated that a linear reduction in actuation force with displacement significantly conditions the emergent motion of the system. It tightens the distribution of foot liftoff positions (when they should all really be the same) and also reduces the spread of step durations, while making the distribution of step durations unimodal. It is worth noting that the linear models here which create such significant improvements are used only at the FTi joint, while the improvements are measured at the ThC joint. These linear

models are also simpler than the piecewise-linear models used in the two-leg platform of Lewinger *et al.* 2006 [27].

These results suggest that the required complexity of actuation-limiting models for stabilizing and conditioning SCASM-based control may be relatively simple in general. This is evidence of the low computational complexity necessary for SCASM control, and suggests that application to a broad range of control problems (and underlying actuation mechanisms) may be both conceptually and practically straightforward for systems which require cyclic sets of coordinated state transitions.

Additionally, it is apparent that adding complexity or conditioning of the underlying plant at one critical module, e.g., by improving the associated muscle model, can significantly improve performance of the entire system without further computational effort associated with other modules. This may simplify the task of the system designer, and also suggests that modulation of the overall system behavior such as that necessary in turning or climbing could be implemented as modulation of one or a few critical modules from a higher-level control mechanism.

ACKNOWLEDGMENT

We thank Brian Taylor for the physical design and construction of the single-leg test platform.

REFERENCES

[1] T. J. Allen, R. D. Quinn, R. J. Bachmann, and R. E. Ritzmann, "Abstracted Biological Principles Applied with Reduced Actuation Improve Mobility of Legged Vehicles," presented at Intelligent robots and systems; 2003 IEEE/RSJ international conference on intelligent robots and systems (IROS 2003), Las Vegas, NV, 2003.

[2] S. A. Bailey, J. G. Cham, M. R. Cutkosky, and R. J. Full, "Comparing the Locomotion Dynamics of the Cockroach and a Shape Deposition Manufactured Biomimetic Hexapod," presented at International symposium on experimental robotics, Waikiki, HI, 2000.

[3] M. Boggess, R. Schroer, R. Quinn, and R. Ritzmann, "Mechanized Cockroach Footpaths Enable Cockroach-like Mobility," presented at International conference on robotics and automation; 2004 IEEE, New Orleans, La., 2004.

[4] T. E. Wei, R. D. Quinn, and R. E. Ritzmann, "A CLAWAR That Benefits From Abstracted Cockroach Locomotion Principles," presented at Climbing and walking robots Conference, Madrid, Spain, 2004.

[5] K. S. Espenschied and R. D. Quinn, "Biologically-Inspired Hexapod Robot Design and Simulation," presented at AIAA Conference on Intelligent Robots in Field, Factory, Service and Space, Houston, Texas, 1994.

[6] K. S. Espenschied, R. D. Quinn, R. D. Beer, and H. J. Chiel, "Biologically based distributed control and local reflexes improve rough terrain locomotion in a hexapod robot," *Robotics and autonomous systems*, vol. 18, pp. 59 (6 pages), 1996.

[7] F. Pfeiffer, H. J. Weidemann, and J. Eltze, "The TUM Walking Machine. - In: Intelligent Automation and Soft Computing," in *Trends in Research, Development and Applications*, vol. 2: TSI Press, 1994, pp. 167-174.

[8] A. Buschmann, "Home of Tarry I & II: design of the walking machine Tarry II," 2000.

[9] B. Gassmann, K.-U. Scholl, and K. Berns, "Behavior control of LAURON III for walking in unstructured terrain," presented at Intl. Conference on Climbing and Walking Robots (CLAWAR '01), Karlsruhe, Germany, 2001.

[10] Lewinger, W.A. "Insect-Inspired, Actively Compliant Robotic Hexapod," M.S. Thesis, Department of Electrical Engineering and Computer Science, Case Western Reserve University, Cleveland, OH, USA. May 2005.

[11] W. A. Lewinger, M. S. Branicky, and R. D. Quinn, "Insect-inspired, actively compliant robotic hexapod," presented at International Conference on Climbing and Walking Robots (CLAWAR), London, U.K., 2005.

[12] H. Cruse, "What Mechanisms Coordinate Leg Movement in Walking Arthropods," *Trends in Neurosciences*, vol. 13, pp. 15-21, 1990.

[13] T. Wadden and O. Ekeberg, "A neuro-mechanical model of legged locomotion: single leg control," *Biological cybernetics*, vol. 79, pp. 161 (14 pages), 1998.

[14] T. Wadden and O. Ekeberg, "A neuro-mechanical model of legged locomotion: quadruped control," presented at International Conference on Climbing and Walking Robots, Portsmouth, 1999.

[15] J. Abbas and R. J. Full, "Neuromechanical interaction in cyclic movements," in *Biomechanics and neural control of posture and movement*, J. M. Winter and P. E. Crago, Eds. New York: Springer-Verlag, 2000, pp. 177-191.

[16] R. K. Josephson, "Contraction Dynamics and Power Output of Skeletal Muscle," *Annual Review of Physiology*, vol. 55, pp. 527-546, 1993.

[17] A. Büschges, J. Schmitz, and U. Bässler, "Rhythmic patterns in the thoracic nerve cord of the stick insect induced by pilocarpine," *Journal of Experimental Biology*, vol. 198, pp. 453-456, 1995.

[18] A. Büschges, C. Ludwar, D. Bucher, S. J, and R. A. DiCaprio, "Synaptic drive contributing to rhythmic activation of motorneurons in the deafferented stick insect walking system," *European Journal of Neuroscience*, vol. 19, pp. 1-7, 2004.

[19] T. Akay, U. Bässler, P. Gerharz, and A. Büschges, "The role of sensory signals from the insect coxa-trochanteral joint in controlling motor activity of the femur-tibia joint.," *Journal of neurophysiology*, vol. 85, pp. 594-604, 2001.

[20] T. Akay, S. Haehn, J. Schmitz, and A. Büschges, "Signals from load sensors underlie interjoint coordination during stepping movements of the stick insect leg.," *Journal of neurophysiology*, vol. 92, pp. 42-51, 2004.

[21] D. Bucher and e. al., "Interjoint coordination in the stick insect leg-control system: The role of positional signaling," *Journal of neurophysiology*, 2002.

[22] D. Bucher, T. Akay, R. A. DiCaprio, and A. Büschges, "Interjoint coordination in the stick insect leg-control system: The role of positional signaling," *Journal of neurophysiology*, vol. 89, pp. 1245-1255, 2003.

[23] D. Hess and A. Büschges, "Role of proprioceptive signals from an insect femur-tibia joint in patterning motoneuronal activity of an adjacent leg," *Journal of neurophysiology*, vol. 81, pp. 1856-1865, 1999.

[24] U. Bässler, "The femur-tibia control system of stick insects – a model system for the study of the neural basis of joint control," *Brain Research Reviews*, vol. 18, pp. 207-226, 1993.

[25] U. Bassler and A. Buschges, "Pattern generation for stick insect walking movements – multisensory control of a locomotor program," *Brain Research Reviews*, vol. 27, pp. 65-88, 1998.

[26] Ö. Ekeberg, M. Blümel, and A. Büschges, "Dynamic simulation of insect walking," *Arthropod structure & development*, vol. 33, pp. 287 (14 pages), 2004.

[27] W. A. Lewinger, B. L. Rutter, M. Blümel, A. Büschges, and R. D. Quinn, "Sensory Coupled Action Switching Modules (SCASM) generate robust, adaptive stepping in legged robots," in *CLAWAR 2006: 9th International Conference on Climbing and Walking Robots*. Brussels, Belgium, 2006.

[28] V. Yodaiken and M. Barabanov, "A real-time Linux," presented at Linux Applications Development and Deployment Conference (USELINUX), Anaheim, CA, 1997.

[29] A. V. Hill, *First and last experiments in muscle mechanics*. Cambridge [Eng.]: University Press, 1970.

[30] U. Bässler, J. Rohrbacher, G. Karg, and G. Breutel, "Interruption of searching movements of partly restrained front legs of stick insects, a model situation for the start of a stance phase?," *Biological cybernetics*, vol. 65, pp. 507-514, 1991.

[31] H. Fischer, J. Schmidt, and A. Büschges, "Pattern generation for walking and searching movements of a stick insect leg I. Coordination of motor activity," *Journal of neurophysiology*, vol. 85, pp. 341-353, 2001.